

Utilisation of waste cardboard and Nano silica fume in the production of fibre cement board reinforced by glass fibres

Khorami, M., Ganjian, E., Saidani, M., Mortazavi, A., Olubanwo, A. & Gand, A.

Author post-print (accepted) deposited by Coventry University's Repository

Original citation & hyperlink:

Khorami, M, Ganjian, E, Saidani, M, Mortazavi, A, Olubanwo, A & Gand, A 2017, 'Utilisation of waste cardboard and Nano silica fume in the production of fibre cement board reinforced by glass fibres' *Construction and Building Materials*, vol. 152, pp. 746-755.

<https://dx.doi.org/10.1016/j.conbuildmat.2017.07.061>

DOI 10.1016/j.conbuildmat.2017.07.061

ISSN 0950-0618

ESSN 1879-0526

Publisher: Elsevier

NOTICE: this is the author's version of a work that was accepted for publication in *Construction and Building Materials*. Changes resulting from the publishing process, such as peer review, editing, corrections, structural formatting, and other quality control mechanisms may not be reflected in this document. Changes may have been made to this work since it was submitted for publication. A definitive version was subsequently published in *Construction and Building Materials*, [152], (2017) DOI: 10.1016/j.conbuildmat.2017.07.061

© 2017, Elsevier. Licensed under the Creative Commons Attribution-NonCommercial-NoDerivatives 4.0 International

<http://creativecommons.org/licenses/by-nc-nd/4.0/>

Copyright © and Moral Rights are retained by the author(s) and/ or other copyright owners. A copy can be downloaded for personal non-commercial research or study, without prior permission or charge. This item cannot be reproduced or quoted extensively from without first obtaining permission in writing from the copyright holder(s). The content must not be changed in any way or sold commercially in any format or medium without the formal permission of the copyright holders.

This document is the author's post-print version, incorporating any revisions agreed during the peer-review process. Some differences between the published version and this version

may remain and you are advised to consult the published version if you wish to cite from it.

1 ***Utilisation of waste cardboard and Nano silica fume in the production***
2 ***of fibre cement board reinforced by glass fibres***

3 Morteza Khorami^{1*}, Eshmaeil Ganjian¹, Azamalsadat Mortazavi¹, Messaoud Saidani¹, Adegoke Olubanwo¹,
4 Alfred Gand¹

5 1: *School of Energy, Construction & Environment*

6 *Faculty of Engineering, Environment & Computing*

7 *Sir John Laing Building*

8 *Much Park Street*

9 *Coventry University*

10 *Coventry*

11 *CV1 2HF*

12 *Tel: +44 (0) 2477659108*

13 *Corresponding Author: morteza.khorami@coventry.ac.uk mrz_khorami@yahoo.com

14 **Highlight** (each bullet point maximum 85 characters)

- 15 - Kraft fibre extracted from waste cardboard can be used in cement board
16 production.
- 17 - Incorporating glass fibres with Kraft fibre can increase flexural strength of
18 cement board.
- 19 - An appropriate amount of Nano Silica Fume can improve properties of
20 cement board.

21

22 **Abstract (100 word limit)**

Acronyms

Glass Fibres (GL), Kraft pulp Fibres (KF), Nano Silica Fume (NSF), Cement Composite Board (CCB)

Water Absorption (WA), Moisture Movement (MM), Flexural Strength (FS) and Scanning Electron Microscopy (SEM)

23 In this research, Glass Fibres (GL), Kraft pulp Fibres (KF) and Nano Silica Fume (NSF) were
24 used to produce Cement Composite Board (CCB).
25 Fifteen groups of mix proportions were produced to investigate the effects of fibre content
26 and size along with the effect of NSF on interaction, bonding and mechanical properties of
27 CCB. Density, Water Absorption, Moisture Movement, Flexural Strength test and Scanning
28 Electron Microscopy observations were conducted. The results showed that some mixes could
29 meet the standard requirements and also the inclusion of GL and NSF into the mix containing
30 KF (extracted from waste cardboard) could enhance the characteristics of CCB.

31

32 **Keywords: cement composite, Cement Board, Glass fibre, Nano Silica Fume, waste**
33 **cardboard**

34 **1 Introduction**

35 Cementitious composites are typically characterised as being brittle with low tensile strength
36 and strain capacities. Fibres are introduced into the matrix to overcome these weaknesses
37 [1,2]. The effectiveness of the fibre reinforcement depends on a number of factors, such as
38 mix preparation process, size, type, geometry, volume and dispersion models of fibres [3,4].

39 Reinforcement fibres not only improve bearing capacity of CCB but also increase fracture
40 toughness of specimens by decreasing the concentrated applied stresses acting on the tip of
41 cracks [5,6].

42 Typical CCBs consist of two or more types of fibres. Some fibres are used to enhance the
43 production process, other may have an important role in increasing the bearing capacity and
44 fracture toughness [3-5]. Thus, the combination of fibres and materials can offer more
45 benefits than the individual entities.

46 Different types of fibres from natural and synthetic sources have been investigated for their
47 suitability in CCB. Cellulose fibres have increasing popularity over the past two decades, due
48 to their renewability, accessibility, low-cost production process, mechanical property, and
49 compatibility with hydrated cement media [1,6-8].

50 The interfacial bond between fibres and hydrated cementitious material has an important role
51 in increasing the bearing capacity of CCB. It is essential to use appropriate fibres and accurate
52 proportion of materials in the mix design to achieve the best efficiency of the product. For
53 example, steel fibres have high tensile strength but are weak in interfacial bonding with
54 hydrated cement products. So, they pull out from the matrix in the first stages of loading
55 before reaching their maximum tensile strength. Several methods have been suggested to
56 increase the interfacial bond such as applying additives, fibre treatment and decreasing the
57 fibre-cement gaps using the vacuum/compressive pressure in the production of CCBs
58 [3,6,9,10].

59 Concerns have been raised regarding the use of CCBs in roofing and cladding applications,
60 mainly due to long-term exposure to aggressive environments. The studies showed that CCBs
61 containing cellulose fibres solely are more sensitive to aggressive ambient conditions and may
62 undergo a reduction in flexural strength and fracture toughness over time. This is associated
63 with a decrease in bearing capacity of CCBs, due to a combination of deterioration of cellulose
64 fibres in the high alkaline environment, fibre mineralisation and volume increasing due to their
65 high water absorption. The high alkaline matrix could easily decompose the lignin and
66 hemicellulose phase that linked individual filaments and resulting in an inhibitory effect on
67 hydration of cement and weakness in fibre structure. In addition, cellulose volume variation
68 could create cracks in the interfacial zone leading to a decrease in fibre pull out strength
69 [1,5,11,12].

70 To provide a less aggressive environment for cellulose fibres, the concentration of hydroxyl in
71 the pore solution needs to be reduced. This could be done by introducing Sulpho Aluminate,
72 Metakaolin or micro silica into the mix [13,14]. The addition of pozzolans such as Nano Silica
73 Fume (NSF) in the cement composite reinforced by natural and polymeric fibres could increase
74 the flexural behaviour of samples [3,11,15].

75 Previous research carried out by the first and second author has shown that the negative
76 effects of lignocellulosic particles cement interaction can be controlled by NSF to enhance
77 durability and flexural strength of CCB [3,5].

78 Following concerns relating to asbestos hazard on human health, in the early 1970s, a global
79 movement was established to remove asbestos fibres from a wide range of products such as
80 asbestos-cement board. One of the most important synthetic fibres used as a replacement for
81 asbestos fibres in cement board production is PVA (Poly Vinyl Alcohol) which can be relatively
82 expensive. It should be taken into account that besides monopolising PVA production
83 technology by several companies, difficulty in accessibility and the high cost of PVA are other
84 adverse factors to using those fibres in some developing countries [1,4,16].

85 In this research, an attempt has been made to investigate the feasibility of producing CCB
86 using a combination of GLs, KFs and NSF, which are relatively cost effective and also readily
87 accessible in most countries.

88 GL has a number of advantageous such as low cost, high tensile strength, and high chemical
89 resistance. It has already been used in cement mortar and demonstrated to have significantly
90 improved the tensile strength and ductility characteristics.

91 The use of normal type GLs incorporated to CCB has shown poor durability due to the
92 following;

93 i) Hydroxyl ions resulted from cement hydration can cause corrosion on the fibres.

94 ii) Precipitation of calcium hydroxide within the GLs, can change the microstructure of
95 fibres from flexible to rigid. This may change the mode of failure from fibre pull out to
96 fibre fracture.

97 iii) Densify the interfacial zone decrease fibres compliance, consequently the non-uniform
98 tensile stress induced by flexural loading would disrupt fibre-bridging effect in cracks.

99 To overcome those above-mentioned problems, it has been suggested to apply “alkali
100 resistant GLs” instead of normal GLs in production of CCB [4,17]. In other words, only alkali
101 resistant GL should be used in cement composite, otherwise, due to chemical corrosion of
102 normal GLs in alkaline media, CCBs can become brittle and weaker through the cement
103 hydration process [18,19]. Currently, alkali resistant GL which is highly resistant to alkalis,
104 acids and corrosion have been developed for reinforcing of cement composite.

105 The use of Nano silica fume in CCB has already been investigated by authors [3] and the results
106 showed that NSF could increase the flexural strength, bending strength and fracture
107 toughness of CCB reinforced by cellulose fibres.

108 In this research, the characteristics of CCB reinforced by Kraft pulp fibres extracted from waste
109 cardboard and alkali resistant GL incorporating NSF have been investigated.

110 **2 Experimental Methodology**

111 **2.1 Materials**

112 The materials used in this research include:

- 113 • Portland cement: Ordinary Portland cement Type I, satisfying the requirement of BS
114 EN 197-1: 2000.

- 115 • Kraft pulp fibres extracted from waste cardboard and refined by using laboratory
 116 refiner equipment.
- 117 • Nano Silica Fume (Grade 999): particle size distribution, physical and chemical
 118 properties of Nano silica have been illustrated in Table1

119 **Table 1:** Physical and chemical properties of Nano silica fume.

Colour	White
Melting Point (°C)	Approx. 1650
Solubility (Water)	Poorly water soluble
Specific Gravity (Water = 1.0)	2.25
Bulk Density (kg/m ³)	95-105
Specific Surface (m ² /g)	50-60
pH Value	3.6-4.5

120

- 121 • Glass Fibres: GL has a three-dimensional structure and is considered as isotropic
 122 materials comprises of a long network of oxygen, silicon and other atoms arranged in
 123 a random fashion. The GLs provided for this research have the non-crystalline
 124 structure, that is, amorphous, with no distinct shape and classed as alkali resistant
 125 glass fibres. They were used in 3mm and 6 mm lengths. The properties of Kraft fibres
 126 extracted from waste cardboard and GL are given in Table 2.

127

128 **Table 2:** Physical properties of the fibres.

129
130
131
132
133
134
135
136
137
138
139
140
141
142

Glass fibres	
Fibre Length (mm)	3 & 6
Filament Diameter (µm)	14-16
Size Content (%) – ISO 1887: 1980	1.0
Moisture (%) – ISO 3344: 1977	0.35 max.
Modulus of Elasticity (GPa)	70-80
High dispersion (filaments per kg)	220 * 106
Kraft fibres	
*Average length (mm)	1.1
**Width (Micron)	20-35
Specific gravity (measured by helium pycnometer)	1.5
Tensile strength	Not specified
Freeness	580

143
144
145
146
147
148
149
150

* Average length obtained from 50 fibres.

**Pulp fibres have ribbon shapes (not cylindrical shapes) with 20-35 micron width.

It should be noted that due to the short length of fibres, measuring the tensile strength was not possible with existing equipment.

The freeness of pulp is designed to give a measure of the rate at which a dilute suspension of pulp (3 g of pulp in 1 L of water) may be drained. The freeness, or the drainage time of pulp is

151 related to the surface conditions and swelling of the fibres. Drainage of unrefined pulp, which
152 is measured as freeness, can give an indication of:

153 • The fibre length. In which, the long fibres have more freeness compared to short
154 fibres.

155 • Damage to fibres during pulping, bleaching or drying. In which, short fibres or fines
156 that are produced during the pulping operation reduce pulp freeness.

157 • The refining energy required to achieve certain slowness during stock preparation.

158 In this study, the freeness test was carried out according to AS/NZS 1301.206s:2002 standard.

159 Freeness is commonly called Canadian Standard Freeness (CSF) because it has been based on

160 the test developed by the Canadian Pulp and Paper Research Institute. For the current study,

161 CSF measured for KFs was around 560-600.

162 **2.2 Production of the specimens**

163 For each mix code, the slurry contains water, cementitious materials and fibres with a high
164 water/cement ratio (i.e. around 3 by the weight of cement) was prepared in a mixer.

165 Then it is poured into a mould and subjected to vacuum and compressive stress of 7 kN/m^2 to

166 form a flat sheet. After the slurry dewatering process, pad (dimensions $180 \times 82 \times 7 \text{ mm}$) was

167 demoulded and cured for 21 days at 95% of relative humidity and air cured in the laboratory

168 for 7 days at a temperature of $20 \pm 2 \text{ }^\circ\text{C}$. The cured specimens were subsequently tested.

169

170 **2.3 Tests**

171 The following subsections outline the tests undertaken in accordance with 1) BS EN 494:2004
172 +A3:2007 (Fibre-cement profiled sheets and fittings – Product specification and test methods)
173 and 2) BS EN 12467:2004 (Fibre-cement flat sheets – Product specification and test methods).

174 **2.3.1 Density**

175 To measure the density of the specimens, a routine laboratory method was used. Initially the
176 mass of the specimens placed in laboratory environment (20 ± 2 °C and 40%-50% RH) for one
177 day was measured. Then to find the volume of the specimens, they were submerged into the
178 water and the displaced water was measured. The result of mass divided by volume was
179 considered as density of the specimens.

180 **2.3.2 Water Absorption**

181 Water absorption was conducted in accordance with ASTM C1186-08 (2012) with reference
182 to ASTM C1185-08 (2012). In this test, to meet the standard requirement, the specimens are
183 dried in an oven at 90 ± 2 °C until constant weight was achieved, then allowed to cool to room
184 temperature and are weighed. The specimen is then submerged in potable water at 20 ± 4 °C
185 for 48 ± 8 hours. Then the specimen is removed and excess water wiped from the surfaces
186 using a damp cloth and weighed again. The weight increased due to submerging the specimen
187 in water is expressed in percentage as the water absorption.

188 **2.3.3 Moisture Movement**

189 Moisture movement was conducted in accordance with ASTM C1186-08 (2012) with reference
190 to ASTM C1185-08 (2012). In this test, the linear deviation in length of the specimen due to
191 moisture absorbed from the surrounding environment is determined. To find the moisture
192 movement according to the standard procedure, the difference between the length of the

193 specimen at Relative Humidity (RH) of 90% and 30%, needs to be divided by the length at 30%
194 RH and the result is expressed in percentage.

195

196 **2.3.4 Flexural strength**

197 Flexural behaviour of the specimens under a three-point load system according to BS
198 EN12467:2004. The specimens were subjected to three-point loading flexural test to failure
199 point which must occur between 30 and 60 seconds of loading time.

200

201 **2.3.5 SEM**

202 The JEOL JSM-6060 LV SEM machine was used for this study. The samples were mounted on
203 stubs and were gold coated using the sputter coater to enhance conductivity. The samples
204 were then placed in the vacuum chamber of the SEM machine and images were captured with
205 different magnifications for the selected specimens. To obtain improved views of the fibres,
206 some images were captured after tilting the samples 75 degrees in relation to the horizontal
207 plane. In the observation, microstructure of fibres, fibre–cement interfacial areas and fibre
208 bonding were studied.

209

210 **2.4 Fibre preparation and mix design**

211 The waste cardboard was shredded into strips 50×5 mm in size. They were then soaked in
212 water and rinsed periodically for two days. The saturated pieces of cardboard were then
213 refined using a laboratory refiner until a uniform Kraft pulp fibres were obtained.

214 The mix design plan is illustrated in Table 3. A broad range of fibre content, fibre size and NSF
 215 content has been investigated in this research. As shown, fifteen groups of mixes were
 216 developed to investigate;

- 217 1. The effect of the size (3 mm and 6 mm) and fibre content (1%, 2% and 3% by the weight of
 218 the cementitious materials).
- 219 2. The effect of NSF content (1%, 2% and 3%) as a replacement for cement on the specimens
 220 reinforced by 3 mm and 6 mm GLs.
- 221 3. The effect of the combination of 3 mm and 6 mm GL with and without NSF.

222 In all mixes, the amount of water was 300 grams which leads to water cementitious materials
 223 ratio of 3 for making the slurry. In Table 3, the amount of Kraft pulp fibres extracted from
 224 waste materials is kept constant (i.e. 4 grams) for all mixes which is 4% by the weight of
 225 cementitious materials. This amount of KF has already been studied by the authors as an
 226 optimum quantity when in combined with polymeric fibres [2,16].

227 In Table 3, the following symbols are defined:

228 K: Kraft pulp fibres extracted from waste cardboard GL: Glass fibres (alkali resistant type)

229 N: Nano silica fume

230

231 Table 3: Details of mix proportions for groups of mix design.

Mi x	Mix Code	N (g)	Cement (g)	GL 3- mm (g)	GL 6-mm (g)
1	K4 (Control)	0	100	0	0
2	K4-GL1-3mm	0	100	1	0

232	3	K4-GL2-3mm	0	100	2	0
233	4	K4-GL3-3mm	0	100	3	0
234	5	K4-GL1-6mm	0	100	0	1
235	6	K4-GL2-6mm	0	100	0	2
236	7	K4-GL3-6mm	0	100	0	3
237	8	K4-GL2-3mm-N1	1	99	1	0
238	9	K4-GL2-3mm-N2	2	98	2	0
239	10	K4-GL2-3mm-N3	3	97	3	0
240	11	K4-GL1-6mm-N1	1	99	0	1
241	12	K4-GL1-6mm-N2	2	98	0	2
242	13	K4-GL1-6mm-N3	3	97	0	3
243	14	K4-GL1-3mm-GL1-6mm	0	100	1	1
244	The 15	K4-GL1-3mm-GL1-6mm- N2	2	98	1	1

245 number after the symbol shows the percentage of the materials by the cement weight. For
 246 example, K4-GL1-3mm-GL1-6mm-N2 means all the specimens of this group contain 4% Kraft
 247 pulp fibre, 1% glass fibre of 3 mm length, 1% glass fibre of 6 mm length and 2% by weight
 248 Nano silica fume.

249 Six replicate specimens were manufactured for each group, allowing multiple tests to be done
 250 and averages taken. The first row of Table 3 (i.e. K4) belongs to the control mix that was
 251 produced only by Kraft pulp fibres, cement and water.

252 It should be noted that during the manufacturing procedures when the slurry was being
253 mixed, it was observed that the specimens containing GL greater than 3% fibre content, the
254 fibres were clustered and clumped hence disrupts the uniformity of fibres throughout the
255 matrix. For this reason, the highest fibre content that was introduced during the slurry mixing
256 was limited to 3% for glass fibres, as shown in Table 3.

257 The mix design shown in Table 3 is a part of the larger table including more than thirty mixes
258 which have been made and tested in this research but after flexural testing of the specimens,
259 it was revealed that flexural strength for many of mixes was less than 6 MPa. So, in this paper,
260 only the results of some mixes which had a flexural strength greater than 6 MPa along with
261 control group are analysed and discussed. For instance, the primary results showed that when
262 the length of GL is 3 mm, the optimum fibre content to gain the highest flexural strength is 2%
263 while for 6 mm length, the corresponding value is 1%. This will be discussed later in other
264 sections. For this reason in Table 3, the effect of NSF on improving the flexural strength of the
265 specimens reinforced by 2% and 1% of 3 mm and 6 mm GL, respectively was chosen to be
266 analysed in this paper.

267

268 **3 Results, Analysis and Discussion**

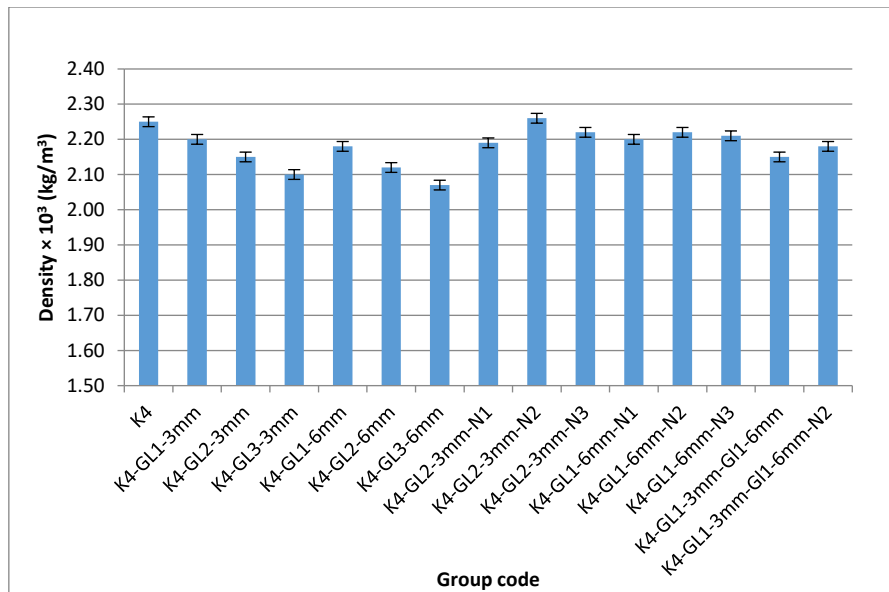
269 Results have been obtained for density, water absorption, moisture movement, flexural
270 behaviour and SEM based on the relevant standards. To show the test precision, error bars
271 are shown on all bar charts (i.e Fig.1 to 4).

272 **3.1 Density**

273 Fig.1 illustrates the average density of the specimens of each group at age 28-day.

274

275



276

277

Fig.1: Average density of the specimens in each group.

278

279 As observed when GL is added to the mix, the density is relatively reduced comparing to the
280 control group (K4). This may be associated with hydrophobic nature of the GLs. Whereas the
281 GLs have little or no affinity for water, they cannot absorb water like Kraft pulp fibres which
282 have hydrophilic nature.

283 Accurate observation of the specimens revealed that GLs are visible on the surface of the
284 specimens reinforced by 3% GLs. This showed that incorporation of 3% GLs into the mix is too
285 high to be embedded properly in the mix resulting in non-uniform dispersion GLs into the mix
286 and higher concentrations being present at the surface that leads to further reduction in
287 density.

288 As seen, embedding NSF into the mix causes an increase in density for all groups reinforced
289 by 3 mm and 6 mm GL's. NSF comprises of amorphous (non-crystalline) silicon dioxide (SiO₂),

290 with very small discrete particles. Large surface area due to very small size particles along with
291 high SiO₂ content makes NSF as a reactive pozzolan which enhances hydration kinetic by
292 increasing the amount of beneficial cement hydration products. NSF reacts with calcium
293 hydroxide crystals formed from the hydration of calcium silicates increasing C–S–H nucleation
294 which leads to the denser microstructure of the matrix. It has been proved that NSF particles
295 act as an activator to promote pozzolanic reactions and filler, thus using the appropriate
296 proportion of NSF can fill the voids containing air and moisture resulting further density for
297 the matrix.

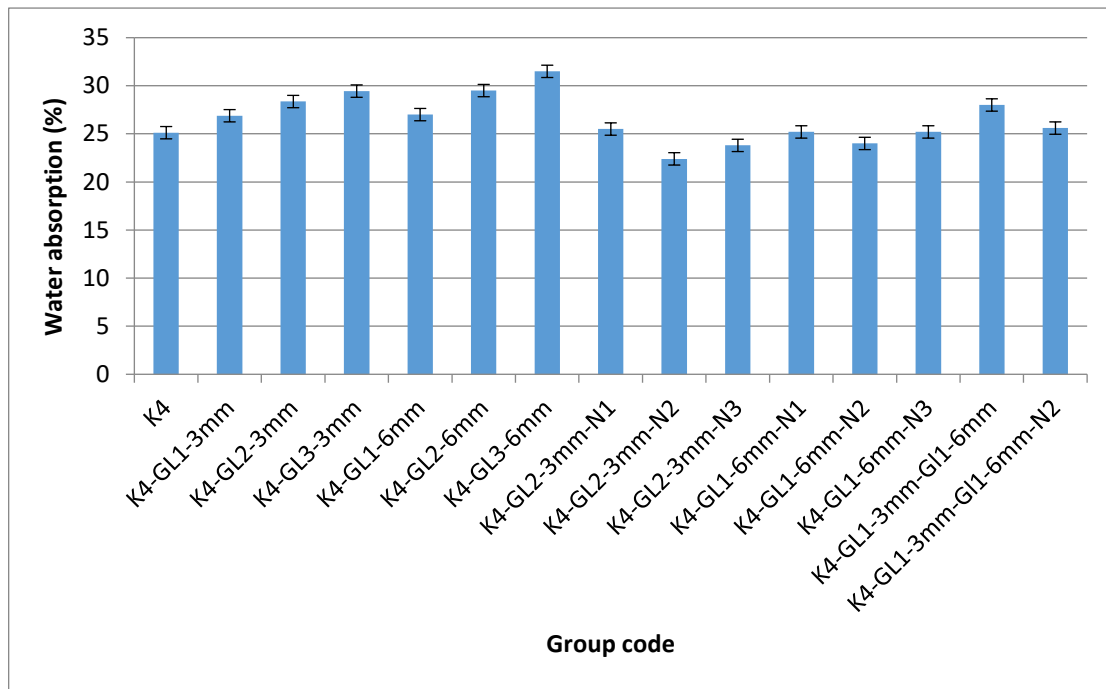
298 As presented in Fig.1, in spite of initial prediction, with increasing the NSF content from 2% to
299 3%, density of the specimens decreases. This may associate with the optimum percentage of
300 NSF. If NSF is used more than 2%, it could have different effects on the matrix, including; 1)
301 the amount of small particles needed for filling the voids would be more than enough hence
302 it may disrupt the appropriate grading in particle size distribution to reach the highest density.
303 2) The amount of NSF required for consuming the calcium hydroxide is more than enough
304 hence the extra NSF will not participate in chemical reactions or filling the voids, so the density
305 will not increase.

306 In this research, variations of density for CCB has been investigated to provide an additional
307 and complementary parameter to determine any links between the density and other
308 observations.

309 **3.2 Water Absorption**

310 Water Absorption (WA) is considered as a key feature for the long life durability of CCBs. Most
311 applications of CCBs require as little WA as possible because it affects the rate of degradation
312 severely.

313 The average WA resulted from each group is presented in Fig. 2.



315

316 Fig.2: The results of average water absorption of the specimens in each group.

317

318 As illustrated in Fig. 2, with increasing the fibre content (3 mm or 6 mm lengths) into the mix
 319 WA increases. With the addition of GLs, the amount of pores within the specimen increases
 320 resulting in more space to enter the water to the specimen. It should be noted that the
 321 mechanism of moisture absorption is different with water absorption in CCB. Moisture
 322 absorption is largely based on capillary action in which the humidity and moisture of the
 323 environment could be sucked into the specimens through tiny pores while in water
 324 absorption, the molecules of water enter and penetrate into the larger voids due to the
 325 hydrostatic pressure of water, rather than sucked by smaller capillaries. In other words, water
 326 absorption could be more susceptible due to water pressure rather than absorbing water due
 327 to capillary action.

328 As presented in Fig. 2, the specimens containing 6 mm GL have a slightly greater affinity for
329 water absorption in comparison to the specimens composed of 3 mm fibres. This could be
330 associated to this fact that the larger 6 mm fibres could create larger pores resulting further
331 porosity.

332 To investigate the effects of NSF on the characteristics of CCB both “fresh” and “hardened”
333 cement composite should be studied considering the following:

- 334 1- NSF could accelerate the hydration of tricalcium silicate (C3S) and C-S-H gel
335 formation. It also aids to remove the non-hydrogen bond OH groups [3,15].
- 336 2- NSF has important effects on the air content in fresh state and on the porosity in the
337 hardened state of the cement composite. Incorporating NSF into the mix, the air
338 content of fresh cement composite increases. This phenomenon affects the viscosity
339 of mix so that with increasing NSF, the viscosity of mix significantly increases
340 because the fine particles of NSF decrease or stop escaping the entrapped air from
341 the fresh mix. In hardened cement composite, NSF decreases the porosity because
342 the pores (i.e. entrapped air) have been surrounded and disjointed by NSF. This
343 finding is consistent with other carried out research [20,21].
- 344 3- Each cement composite mix has a specific capacity of NSF to reach the minimum
345 porosity. As outlined, only some of NSF reacts with hydrated cement products and
346 the rest fills the pores. By filling the pores, both within hydrated cement products
347 and the fibre-cement interfacial zone are filled, the grading of all mixed content is
348 improved and hence the porosity decreases. If the amount of NSF is more than
349 enough for filling the gaps, the extra NSF particles disrupt the grading of mix content
350 resulting in porosity rising.

351 Considering those aforementioned effects, an optimal amount of NSF could provide the
352 lowest porosity for the hardened composite [19,21,22].

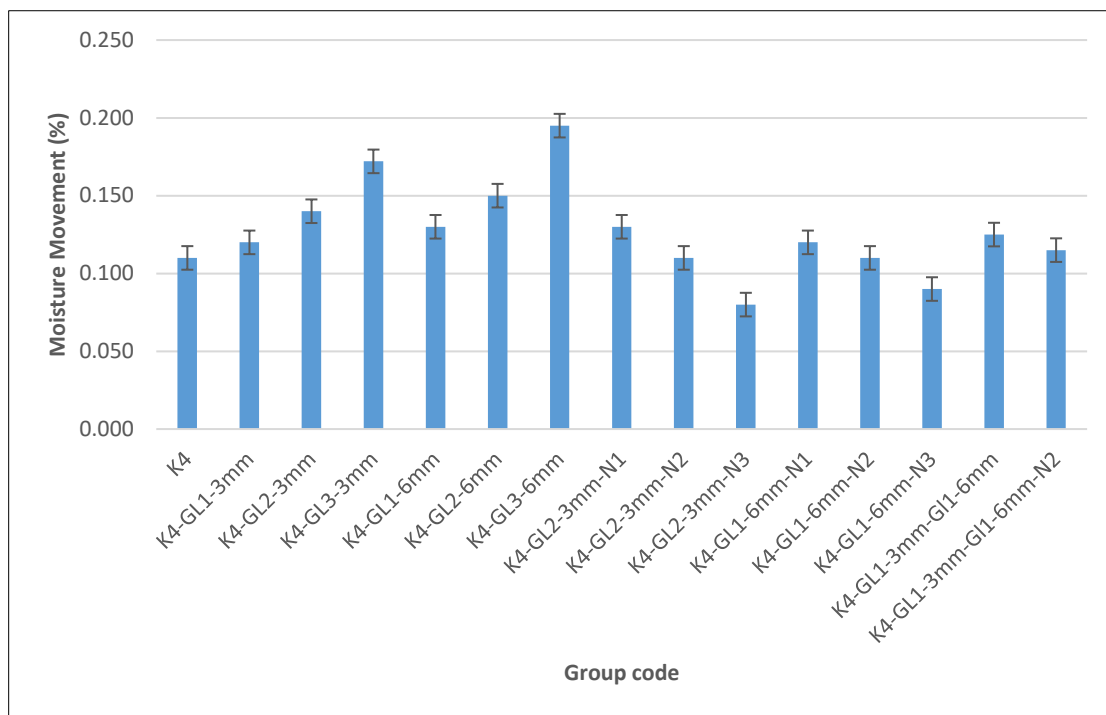
353 As seen in Fig. 2, two different tendencies due to incorporating NSF can be observed in
354 hardened cement composite; increasing the small amount of NSF (i.e. 1%) leads to a decrease
355 in the porosity while the high amount of NSF (i.e. 3%) leads an increase in the porosity. As
356 observed, 2% NSF could be considered as a critical value (optimum proportion) resulting in
357 minimum porosity and minimum water absorption. Referring back to Fig.1, this statement is
358 consistent with the observation that the highest density belongs to the group composed of
359 2% NSF.

360

361 **3.3 Moisture Movement**

362 This test is used to check the appropriateness of the CCB that are exposed to moisture and
363 high humidity. The average moisture movement for all groups is shown in Fig. 3.

364



366

Fig.3: The results of moisture movement for all groups.

367

368

369 Fig. 3 shows that the amount of moisture movement for all groups is less than 0.20% which is
 370 the extremely small amount. CCB is a porous cementitious material containing cellulose fibres
 371 (Kraft pulp) that can absorb moisture and thus increase in size. This could be important for
 372 CCB depends on application purpose and should be in the permitted tolerance range. For most
 373 of the applications such as cladding and external walls, all groups fall in the permitted range
 374 of tolerances.

375 The inclusion of varying proportions and lengths of hydrophobic GLs in the mix can reduce the
 376 moisture movement for all groups compared to control group (K4). However, with increasing
 377 GL content, the moisture movement increases too. As outlined in water absorption, GL can
 378 increased porosity either in the form of small capillaries or creation of larger voids within the
 379 specimen. So, when the moisture is drawn in due to any reason such as capillary action, the

380 Kraft cellulose fibres absorb the moisture and swell leading to an increase in the size of the
381 specimen.

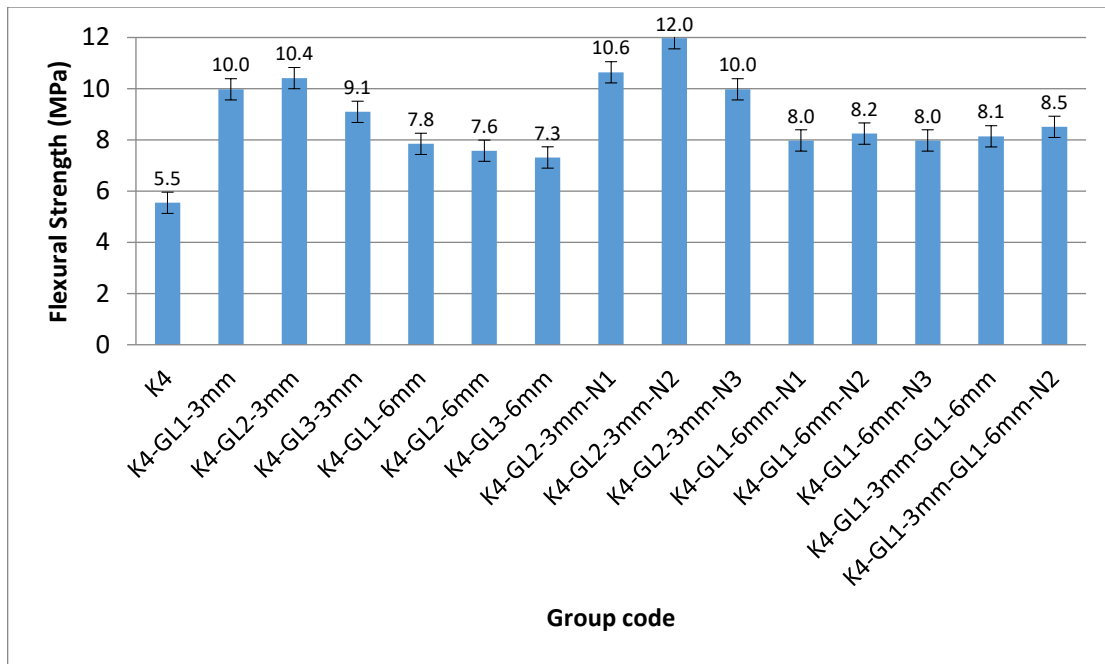
382 The effect of NSF on moisture movement is consistent with the results already outlined in
383 water absorption and density sections with minor differences. As NSF is introduced into the
384 mix, the density and water absorption are affected but both of them show an optimum of 2%
385 NSF to achieve the highest density and the lowest water absorption. As depicted in Fig. 3 with
386 increasing NSF, MM decreases continuously. This may be attributed to the capillary action in
387 which with increasing NSF, the capillary pores that could be considered as pathways for tiny
388 molecules of humidity, are blocked by NSF, consequently, MM decreases. Similar behaviour
389 has already been reported by other researchers [21,22]. The fewer voids constrict the fibres
390 and inhibit their ability to absorb water. The least amount of moisture movement that can be
391 achieved is generally considered as a significant advantage for CCB.

392 The mixes containing 3% of 6 mm GLs demonstrating higher water absorption rather than 3
393 mm GLs due to further porosity resulting from “balling phenomenon” which is described in
394 the next section.

395 **3.4 Flexural testing**

396 Flexural test is the most important mechanical properties of CCBs which has been pointed by
397 all relevant standards. The results of the flexural test on the specimens after 28 days curing
398 are shown in Fig. 4.

399



400

401

Fig.4: The average flexural strength of the specimens for each group.

402

The last experiment conducted on the specimens was the flexural test. It is believed that the

403

specimens may have been interfered by the tests conducted previously (i.e. WA and MM).

404

This could demonstrate the flexural strength of the specimens in the worst case by simulating

405

the real environmental conditions such as cycles of high-low humidity and wet-dry exposure

406

experienced by the specimens.

407

Fig. 4 shows;

408

- The incorporation of GLs (3 mm or 6 mm) into the mix increases the flexural strength

409

in all groups comparing to control mix (K4). This is due to mechanical characteristics

410

of GL such as tensile strength and modulus of elasticity which could improve bearing

411

capacity of CCB.

412

- The effect of 3 mm length GLs in enhancing flexural strength is greater than 6 mm.

413

- The maximum flexural strength of the specimens reinforced by 6 mm length GLs solely

414

belongs to 1% fibre content which is considerably lower than 3 mm. The dominant

415 reason to decrease the flexural strength is associated with balling (clumping)
416 phenomenon; When the percentage of 6 mm length of GLs in the mix increases more
417 than optimum, the fibres cannot disperse uniformly throughout the mix and clump
418 together in the form of ball shape, forming bundles of accumulated individual fibres
419 with low specific contact area, resulting in weak points in matrix. This phenomenon
420 disrupts the crack-bridging effect to stop cracks, whereas the initiation of those cracks
421 is made more likely by the greater extension of unreinforced areas found in the
422 specimens. This will be discussed later in microstructure section.

423 - As seen, when the length of GL is 3 mm, the optimum fibre content to gain the highest
424 flexural strength is 2% while for 6mm length, the corresponding value is 1%. For this
425 reason, the effect of NSF on improving the flexural strength of the specimens was
426 studied only on 2% fibre content for 3 mm GL and 1% fibre content for 6mm length.

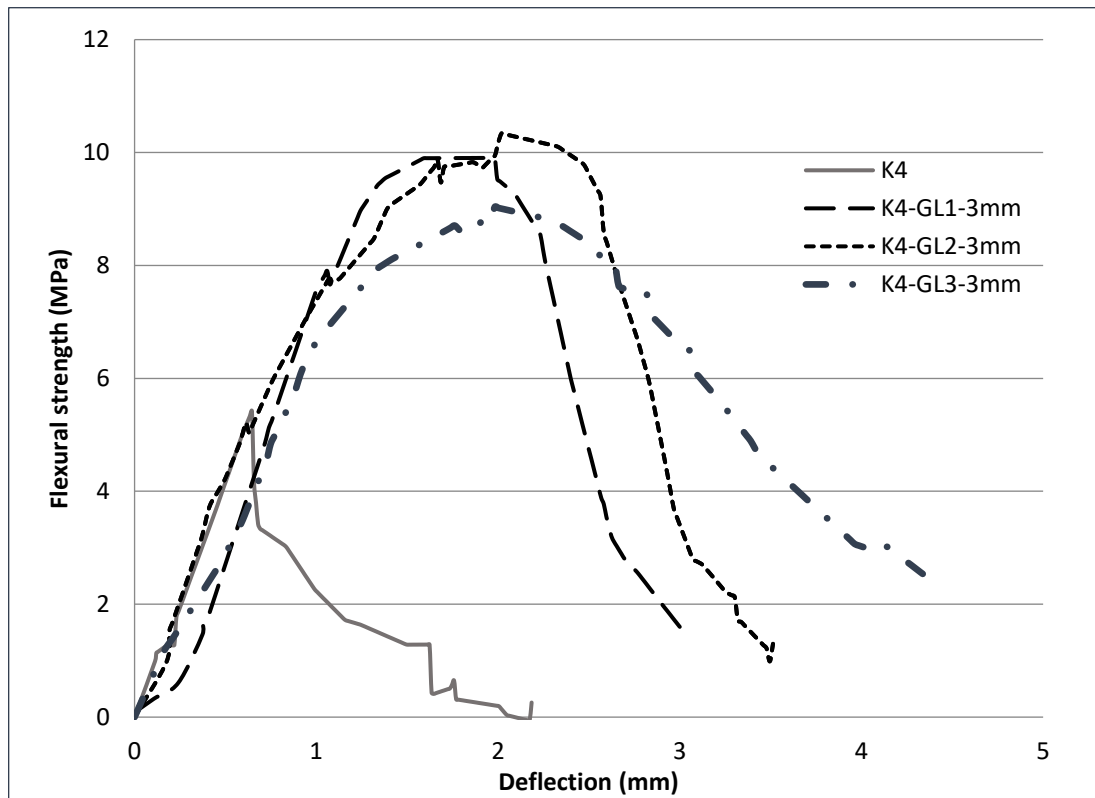
427 - The NSF has a positive effect on rising the flexural strength of the specimens
428 reinforced by GLs. The optimum amount of 2% NSF led to the maximum flexural
429 strength of 12 MPa for group K4-GL2-3mm-N2. This is due to bonding improvement
430 within fibre-cement interfacial zone, decreasing porosity and uniform dispersion of
431 fibres into the mix. This will be illustrated by microstructural studies of the specimens
432 in the next section.

433 - The simultaneous use of 3 mm and 6 mm length GLs couldn't improve the flexural
434 strength considerably comparing to the specimens reinforced by 3 mm or 6 mm solely.

435 To study the flexural behaviour of the specimens during the loading procedure Figs. 5 to 7
436 illustrate the effects of the percentage (1%, 2% and 3%) of GL content, length (3 mm and 6
437 mm) of GL and NSF content (1%, 2% and 3%).

438 Fig. 5 compares the mid-span deflection against the flexural stress of the specimens reinforced
439 by different percentage of 3 mm length of GLs.

440



441

442 Fig.5: The effect of fibre content (1%, 2% and 3%) of GL-3mm on flexural behaviour.

443

444 As seen in Fig. 5, adding GL to the mix increases not only the area under the curve which is
445 directly related to fracture toughness but also the flexural strength of the specimens. Although
446 the energy absorption (which is identified by the area under the curve) for all groups
447 reinforced by GL is approximately identical, the flexural strength of K4-GL2-3mm reaches to
448 10.4 MPa which is the greatest values in comparison to others. In other words, within the
449 range of fibre content studied, the best proportion of GL for the specimens containing 4% of
450 Kraft fibres is 2%, which provides the maximum of 10.4 MPa flexural strength. The mechanical

451 properties of GL, particularly, tensile strength plays an important role in bearing capacity of
452 the specimens. This will be discussed later under microstructure study subsection.

453 As seen in fig.5, the plots for the specimens containing GLs indicate several steps or
454 fluctuations (serrated line). This is associated with initiation of microcracks due to fibre pull
455 out or fibre breaking. The applied stress is then redistributed and is taken by other fibres,
456 allowing further increases in load bearing. In other words, when a micro-crack is arrested by
457 fibre crack bridging mechanism, the stress at interfacial zone rises until either the fibre breaks
458 or pull out, whichever reaches maximum bearing capacity earlier. Then by forming the cracks,
459 the stress is released immediately (serrated line in the plots) and by redistribution of stress,
460 new micro-cracks appear elsewhere. This mechanism continues until the micro-cracks join
461 with each other, forming a visible crack. Previous research carried out by the first author
462 showed that redistribution of stress after initial cracks could be observed in CCB reinforced by
463 Kraft fibres and polymeric fibres [2,3,16]. The visible cracks are initiated at mid-span where
464 maximum tensile stresses are initiated in the component fibres. This stress is called “Bend
465 Over Point”. From this point, the stress keeps rising but with a different slope. As the crack
466 width increases, the specimen elongation increases then the load is being taken by the fibres
467 bridging the cracks until subsequent total failure occurs. In addition, the introduction of GLs
468 within the mix could increase the ductility of the specimens in the threshold of failure about
469 three times in comparison to the specimens wholly reinforced with KFs. This is also associated
470 with the high tensile strength and longer anchorage length of GLs compared to KFs.

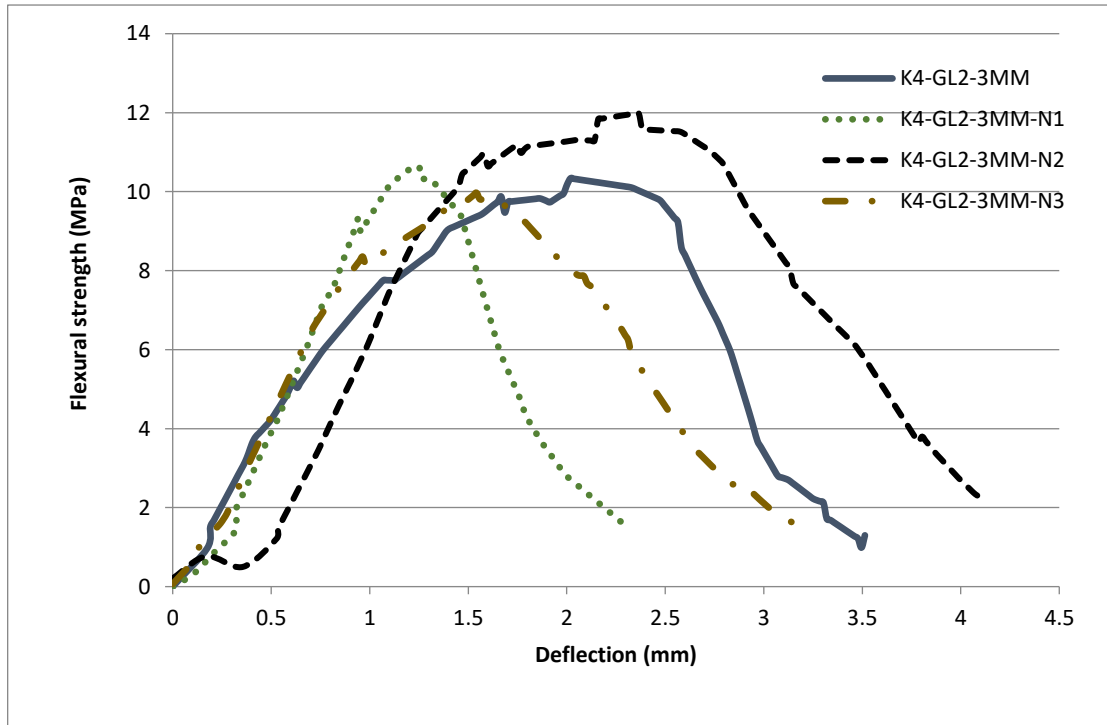
471 As outlined in Fig. 4, the highest flexural strength belongs to K4-GL2-3mm. So, this group was
472 chosen to be investigated by inserting NSF in the matrix.

473 Fig. 6 presents the effect of various percentage of NSF on the flexural performance of the
474 specimens reinforced by only 2% GL-3mm.

475

476

477



478

479 Fig.6: The effect of NSF on the flexural performance of the specimens reinforced by 2% GL-
480 3mm.

481

482 As illustrated in Fig. 6, introduction of NSF to a mix containing 4% KF's and 2% GL's only offers
483 positives strength characteristics (fracture toughness and flexural strength) when 2% NSF is
484 used. This is associated with the optimum percentage of NSF. It seems that 1% NSF is not
485 enough to fill the voids or acts as an activator to enhance the cement hydration process.
486 Similarly, 3% NSF seems to be more than enough for the mix that can interfere with the
487 cement. Excessive use of NSF results in poor-graded particle size distribution within the
488 hydrated cement products, fillers and fibres, disrupts both the mechanical and physical

489 properties of CCB. As observed, 2% of NSF could meet the physical and mechanical
490 requirements in terms of both filling the voids that lead to porosity reduction and activating
491 calcium hydroxide to produce Calcium Silicate Hydrate (C-S-H). This statement is consistent
492 with the results of density outlined in Fig1. In other words, the optimum percentage of NSF
493 can enhance the grading of ingredients in terms of particle size distribution and pozzolanic
494 activator to reach the highest density, lowest water absorption and appropriate moisture
495 movement as outlined in the previous sections.

496

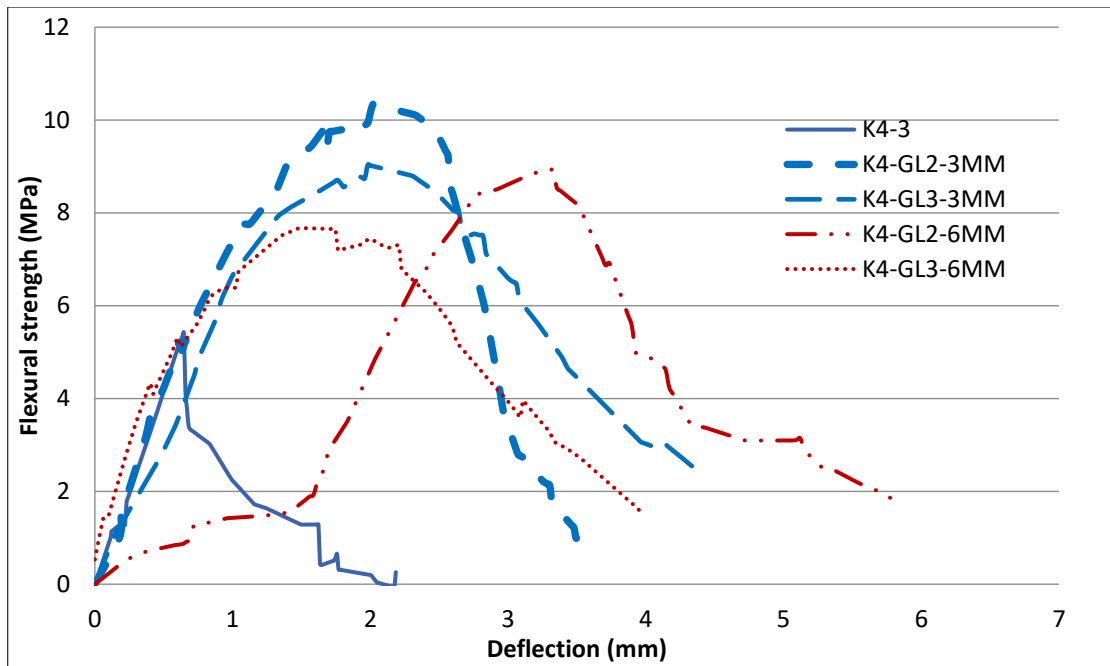
497

498

499 Fig. 7 illustrates the effects of GL fibre's length (i.e. 3 mm and 6 mm) on the flexural
500 performance of CCBs.

501 As seen in Fig. 7, the flexural strength of specimens reinforced by longer GLs (i.e. 6 mm) are
502 weaker than the specimens reinforced by 3 mm lengths of GLs. The maximum flexural strength
503 experienced by the specimens reinforced by 3 mm GL's are 10.3 MPa and 9 MPa for 2 % and
504 3% fibre content respectively while the corresponding values for 6mm GL's are 8.9 MPa and
505 7.7 MPa respectively. As observed in Fig. 7, fracture toughness which relates to the area under
506 the curve for the specimens reinforced by 3mm GL's are relatively larger than the counterpart
507 specimens reinforced by 6 mm GLs. This behaviour is attributed to the interaction of the
508 relatively longer fibres with each other resulting in "balling phenomenon" which in turn
509 reduces the bearing capacity of the specimens.

510



511

512 Fig.7: The effect of GL's length on flexural performance of the specimens.

512

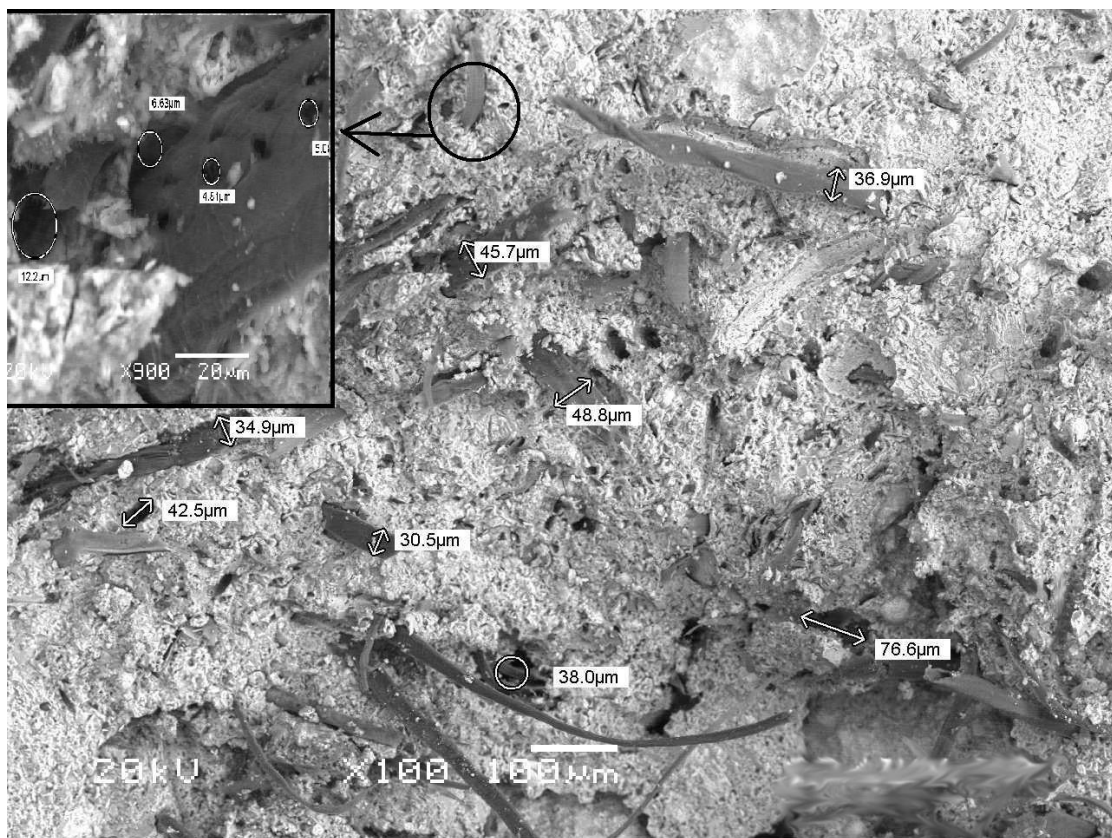
513

514 Surrounding fibres by hydrated cement products could provide enough anchorage length for
 515 transferring the load by the bridge-cracking effect. In spite of this fact, during manufacturing
 516 process of the specimens, the long GLs (i.e. 6 mm) could not be distributed uniformly in the
 517 mix and clumped with each other or with cellulose fibres forming a ball shape twisted/tied
 518 fibres (i.e. balling phenomenon) that could be considered as the voids in the matrix. In other
 519 words, uniform fibre dispersion is essential in the matrix because the cracks initiate and
 520 advance from sections of a composite that has either fibre clumping or larger fibre free areas.

521 4 Microstructure study (SEM)

522 Microstructure studies of three samples including K4, K4-GL2-3mm and K4-GI-3mm-N2 were
 523 carried out using SEM. The fibres and materials which have been focused on this study include;
 524 Kraft fibres, Glass fibres and Nano silica fume.

525 Fig. 8 indicates the fracture surface of KFs reinforced CCB in group K4, displaying Kraft fibres
526 dispersion and the positions of some Kraft fibres after pulling out across the section. As
527 seen, both types of failure including fibre breaking and fibre pull out are visible in Fig. 8. This
528 confirms that there is a relatively strong bond in the interfacial zone within Kraft fibres and
529 hydrated cement products. If the anchorage length of Kraft fibres falls in appropriate ranges,
530 the mechanism of failure tends to pull out rather than breaking the fibres [1,16]. The voids
531 shown in Fig. 8 have the same size as the fibres diameter confirming that the failure occurs
532 due to a pull out mechanism. Apart from the voids created by pulling the fibres, there are
533 other voids visible in Fig. 8 which have been formed in some part of unreinforced matrix due
534 to partial compaction



535
536 Fig.8: Interfacial zone within fibres and hydrated cement products in K4 (X100 & X900
537 magnifications).

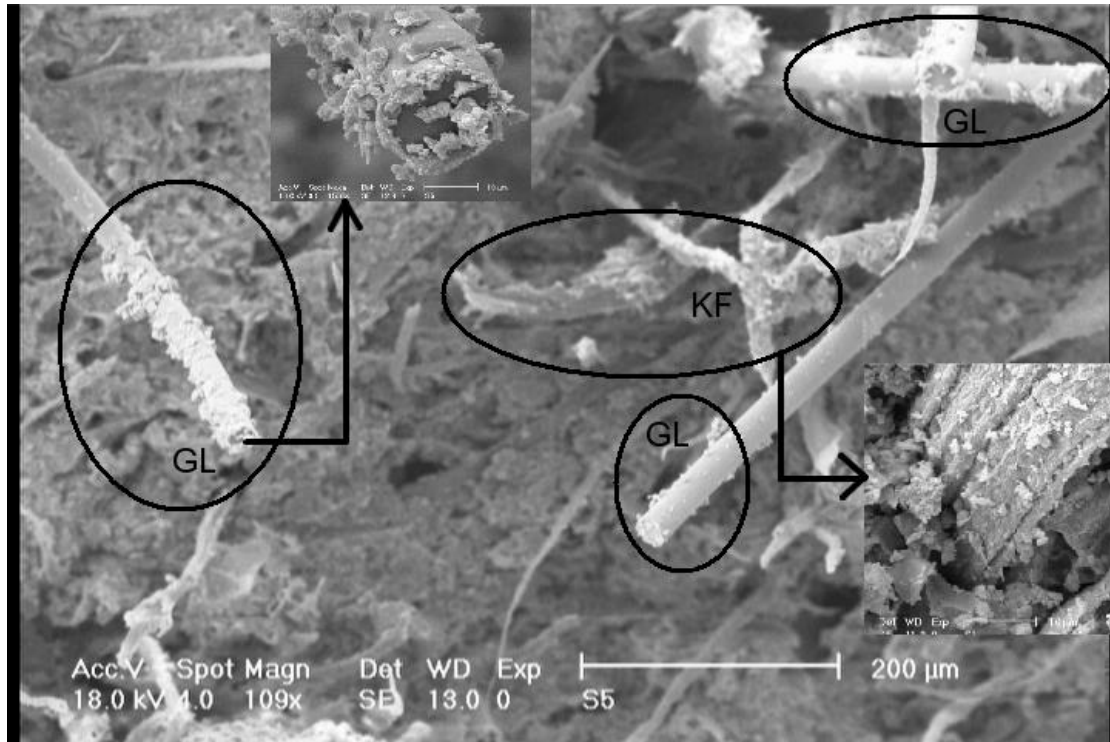
538

539 As seen in Fig. 8, the entire section has been dominated by calcium silicate hydrate (C-S-H)
540 which are connected and surrounded by numerous needle shaped hydrates [20,21]. C-S-H is
541 considered as the principle binding product within hydrated cement product.

542 Fig. 9 depicts a cross section of sample K4-GL2-3mm in which the cylindrical GL's have been
543 covered by the small amount of hydrated cement products (magnified at top left inset of Fig.
544 9) while ribbon shape KFs (magnified at the bottom right inset of Fig. 9) have been almost
545 fully covered. Primarily, the most important cement hydrated products which are formed
546 around GLs are ettringite needle shaped crystals that are formed from the reaction between
547 calcium aluminate and calcium sulphate of cement. The formation of ettringite needle shaped
548 crystals in the vicinity of polymeric fibres has already been reported by other researchers [4,7].

549 Several phenomena occur at early stages of hydration process. In addition to the plateau of
550 the gel pore water intensity, the rate of consumption of capillary water is changed. As C-S-H
551 grows, the capillary pores in the vicinity of GLs increase because of the hydrophobic
552 property of GLs. The excess water that is not consumed in the hydration process will
553 evaporate and leave the space within the matrix and thus increase the porosity. The porosity
554 can cause a reduction in bearing capacity of the specimen and also increase water
555 absorption as already discussed.

556



557

558 Fig.9: Hydrated cement products distribution on GL's and KF's (X100 and X1600
 559 magnifications).

560

561 As illustrated in Fig. 9, fibres are distributed randomly through the cross section. Some fibres
 562 are protruding outwards from the composite and some of them lay lengthways along the
 563 fractured face of the composite. Obviously, all distributed fibres can contribute in controlling
 564 the shrinkage cracks while only some of them which are distributed on the longitudinal axis of
 565 CCB could contribute in the flexural bearing capacity of CCB.

566 As seen, in spite of the KFs, the lateral surface of the GLs is smooth and contains only some
 567 randomly distributed minute (i.e. 1.2 - 2 μ m) imperfections or debris. It seems that due to
 568 hydrophobic characteristics coupled with the smooth surface of GLs, the tendency of
 569 hydrated cement products for placing on the GLs is lower than KFs. Although signs of cement
 570 hydration products on the glass fibre are observable, interfacial bonding within GLs and
 571 hydrated cement cannot be as strong as KFs.

572 It is clear that GLs are not as hydrophilic (wetable) as the KFs. Wetting occurs due to
573 intermolecular interactions when the two molecules are brought together [4]. As seen in Fig.
574 9, although rough (irregular) surface and hydrophilic property of KFs could create a relatively
575 strong bonding in interfacial zone, the slight adhesive bonding within GLs and the hydrated
576 cement products are still observed.

577 Generally, two types of bonding occur simultaneously at the fibre-cement interfacial zone
578 described as, a) Mechanical interlocking resulted from friction within fibres and hydrated
579 cement products and b) Chemical bonding which largely includes strong covalent O-H bonds
580 and weaker Hydrogen bond.

581 It should be noted that polymeric fibres with hydrophobic properties cannot establish any
582 strong chemical bonding with hydrated cement products unless the structure of the polymeric
583 fibres has metal ions to form an ionic bond in the interfacial zone.

584 Since the mechanical characteristics of glass fibres in terms of elasticity modulus and tensile
585 strength are substantially greater than KFs, it can increase flexural strength and fracture
586 toughness of CCBs when an appropriate proportion of GLs is embedded into the mix. It should
587 be noted that depending on the anchorage length, both fibre-breaking and pull out
588 mechanisms have been observed in KFs while the high tensile strength of GLs justifies fibre
589 pull out predominance.

590 Fibres have an important role in transferring the load. As cracks progress, while the fibres
591 carrying the maximum stress, fibre pull out is being occurred gradually. During this loading
592 procedure, the main factor that ultimately controls this compromise is interfacial bond, not
593 the properties of individual materials working alone [1,4,5].

594 Both Figs. 8 and 9, illustrate that the intensity of porosity in the fibre-cement interfacial zone
595 is greater than other zones. This porosity could be considered as tiny cracks in the vicinity of

596 fibres and could be attributed to fibre properties specifically water absorption. Water
597 absorption is one of the intrinsic properties of Kraft pulp fibres which causes considerable
598 volumetric changes in the structure of the cellulose fibres. This increases the water-cement
599 ratio in the interfacial zone which has a negative effect on fibre-cement bonding due to
600 differential drying shrinkage of the matrix. As a consequence, it can generate the cracks and
601 cause a reduction in flexural strength.

602 As already mentioned, in this research, to reduce porosity in the vicinity of the fibres, NSF was
603 used as shown in Fig. 10.



604

605 Fig.10. Effect of NSF on the microstructure of CCBs containing KF's and GL's. (x200 and
606 x1000 magnifications).

607

608 As seen in Fig. 10, both pozzolanic reactions and filler action cause GLs (highlighted at the
609 right side of Fig. 10) and KFs (left side of Fig. 10) are covered by hydrated cement products
610 particularly Calcium Silicate Hydrate (C-S-H).

611 Pozzolanic reactions of NSF ensures that calcium hydroxide (CH, also called “portlandite”
612 which is considered as less-beneficial hydration products) is consumed rapidly to increase C–
613 S–H nucleation which has the main role in providing the strength in a cement matrix. The
614 reduction of CH could also improve the durability of cellulose fibres in alkaline media [3].

615 Pozzolanic reaction of NSF is also caused a reduction in the Ca/(Si + Al) ratio which can improve
616 hydration products. It has been demonstrated that less than one-third of the calcium
617 hydroxide (portlandite) reacts with NSF to form C-S-H. The rest of the calcium comes from the
618 C-S-H that has already been produced in the early stages of hydration process by the reaction
619 of Alite (C₃S) before NSF promote pozzolanic reactions [20].

620 Muller *et al.* [20] showed that NSF has an important effect on reducing the porosity by
621 consuming the water in both interlayer and gel pore spaces of C–S–H. C–S–H can be classified
622 as “solid C–S–H” and “bulk C–S–H”. The “solid C–S–H” includes the Ca–O backbone layers with
623 SiO₂ tetrahedral and the interlayer water in between but excludes the water and any
624 hydroxyls on the outer surface of the stacked layers. The “bulk C–S–H” is the C–S–H inclusive
625 of the gel water [20]. Both solid and bulk resulting from NSF can decrease the porosity and
626 consequently, lead to increasing fibre-cement interface bonding.

627 It is well known that by reducing the porosity, water absorption and moisture movement
628 decrease, whereas density increases. The more hydrated products deposit on glass and Kraft
629 fibres, the more interfacial bonding is created, leading to the greater flexural strength and
630 fracture toughness.

631 The capillary pores (also called “interhydrate pores”) that are formed with growing C–S–H
632 needles (hydration process) plateau rapidly with no further decrease. The reservoir of capillary
633 water which has already been absorbed by cellulose fibres (i.e. KFs) reaches the interhydrate

634 pores over the hydration process and reacts with the silica fume that has already been placed
635 in capillary pores [20,21].

636 As seen in Fig. 10, many of capillary voids or even large pores have not been filled by water
637 that needed to be discussed from a viewpoint of porosity. Porosity would have a negative
638 effect on durability and strength if the tiny voids are linked and joined together resulting in
639 increasing penetrability of CCB. In other words, the capillary pores which are not connected
640 or joined with each other cannot affect the durability of CCB. They can even increase fracture
641 toughness and also the durability of composite against environmental condition such as
642 freeze-thaw cycling.

643 **5 Concluding remarks**

644 The results of this research showed that discrete alkali resistant glass fibres have an
645 appropriate potential to be used in combination with Kraft pulp fibres, cement and Nano-silica
646 fume to produce CCB's. The following can be deduced from the study:

- 647 1. Flexural strength of CCBs increases substantially as GLs are introduced into the
648 mix containing only KFs .
- 649 2. GLs with a length of 3 mm showed better consistency with other ingredients in
650 the mix and could improve flexural strength, water absorption and moisture
651 movement.
- 652 3. The most impressive flexural strength results (12 MPa) belong to the group "K4-
653 GL2-3mm-N2" which comprises of 4% KF's, 2% of 3 mm length GL's, and 2% NSF.
654 The corresponding values for water absorption, moisture movement and density
655 of that group are 22.5%, 0.11% and 2260 kg/m³, respectively.

- 656 4. There is a particular limit for adding GLs into the mix depending on fibre size,
657 manufacturing process and the amount of other ingredients. Extra fibres cause
658 negative effects, such as non-uniform fibre dispersion or clumping fibres which
659 could weaken CCB's properties. In this study, laboratory observation indicates
660 that 3% of cement weight is the maximum limit for incorporating of glass fibre
661 into the mix.
- 662 5. Microstructural studies showed that the pores in the vicinity of GLs are more than
663 the counterpart KFs.
- 664 6. Incorporating an appropriate percentage of NSF into the mix can improve the
665 flexural strength and reduce the porosity of the specimens. Pozzolanic reaction
666 along with filler action of NSF form a stronger bonding at fibre-cement interfacial
667 zone and also improve the durability of CCB by decreasing the permeability of the
668 matrix.

669 **6 Acknowledgements**

670 The authors would like to thank Coventry University for providing the required facilities for
671 this research.

672 **7 References**

673 [1] Khorami M, Sobhani J. An experimental study on the flexural performance of agro-waste cement
674 composite boards. *Int J Civ Eng* 2013;11:207-16.

675 [2] Khorami M, Ganjian E, Srivastav A. Feasibility Study on Production of Fiber Cement Board Using
676 Waste Kraft Pulp in Corporation with Polypropylene and Acrylic Fibers. *Materials Today: Proceedings*
677 2016;3:376-80.

678 [3] Khorami M, Ganjian E. The effect of limestone powder, silica fume and fibre content on the
679 flexural behaviour of cement composite reinforced by waste Kraft pulp. *Constr Build Mater*
680 2013;46:142-9.

- 681 [4] Ardanuy M, Claramunt J, Toledo Filho RD. Cellulosic fibre reinforced cement-based composites: a
682 review of recent research. *Constr Build Mater* 2015;79:115-28.
- 683 [5] Khorami M, Ganjian E. Comparing the flexural behaviour of fibre–cement composites reinforced
684 bagasse: Wheat and eucalyptus. *Constr Build Mater* 2011;25:3661-7.
- 685 [6] Pacheco-Torgal F, Jalali S. Cementitious building materials reinforced with vegetable fibres: A
686 review. *Constr Build Mater* 2011;25:575-81.
- 687 [7] Xie X, Zhou Z, Jiang M, Xu X, Wang Z, Hui D. Cellulosic fibres from rice straw and bamboo used as
688 reinforcement of cement-based composites for remarkably improving mechanical properties.
689 *Composites Part B: Engineering* 2015;78:153-61.
- 690 [8] Mohammad Kazemi F, Doosthoseini K, Ganjian E, Azin M. Manufacturing of bacterial nano-
691 cellulose reinforced fibre– cement composites. *Constr Build Mater* 2015;101:958-64.
- 692 [9] Ashori A, Tabarsa T, Valizadeh I. Fiber reinforced cement boards made from recycled newsprint
693 paper. *Materials Science and Engineering: A* 2011;528:7801-4.
- 694 [10] Torkaman J, Ashori A, Momtazi AS. Using wood fiber waste, rice husk ash, and limestone powder
695 waste as cement replacement materials for lightweight concrete blocks. *Constr Build Mater*
696 2014;50:432-6.
- 697 [11] Sonphuak W, Rojanarowan N. Strength improvement of fibre cement product. *International*
698 *Journal of Industrial Engineering Computations* 2013;4:505-16.
- 699 [12] Hakamy A, Shaikh F, Low IM. Effect of calcined nano clay on microstructural and mechanical
700 properties of chemically treated hemp fabric-reinforced cement nanocomposites. *Constr Build Mater*
701 2015;95:882-91.
- 702 [13] Marikunte S, Aldea C, Shah SP. Durability of glass fibre reinforced cement composites:: Effect of
703 silica fume and metakaolin. *Adv Cem Based Mater* 1997;5:100-8.
- 704 [14] Asokan P, Osmani M, Price AD. Assessing the recycling potential of glass fibre reinforced plastic
705 waste in concrete and cement composites. *J Clean Prod* 2009;17:821-9.
- 706 [15] Aly M, Hashmi MSJ, Olabi AG, Messeiry M, Abadir EF, Hussain AI. Effect of colloidal nano-silica on
707 the mechanical and physical behaviour of waste-glass cement mortar. *Mater Des* 2012;33:127-35.
- 708 [16] Ganjian E, Khorami M. Application of Kraft and Acrylic Fibres to Replace Asbestos in Composite
709 Cement Board. 2008:52-61.
- 710 [17] Ali M, Majumdar AJ, Singh B. Properties of glass fibre cement—the effect of fibre length and
711 content. *J Mater Sci* 1975;10:1732-40.
- 712 [18] D.D. T. Creep characteristics of glass reinforced cement under flexural loading. *Cement and*
713 *Concrete Composites* 1995;17:267-79.
- 714 [19] Enfedaque A, Gálvez J, Suárez F. Analysis of fracture tests of glass fibre reinforced cement (GRC)
715 using digital image correlation. *Constr Build Mater* 2015;75:472-87.

- 716 [20] Muller A, Scrivener K, Skibsted J, Gajewicz A, McDonald P. Influence of silica fume on the
717 microstructure of cement pastes: New insights from 1 H NMR relaxometry. Cem Concr Res
718 2015;74:116-25.
- 719 [21] Vinayag MB, Aleem MA, Tharrini J, Roja SY. REVIEW ON STRENGTH AND DURABILITY
720 CHARACTERISTIC OF GEOPOLYMER CONCRETE WITH MACRO SILICA, NANO SILICA. 2015.
- 721 [22] Pourjavadi A, Fakoorpoor SM, Khaloo A, Hosseini P. Improving the performance of cement-based
722 composites containing superabsorbent polymers by utilisation of nano-SiO₂ particles. Mater Des
723 2012;42:94-101.
- 724